Molecular and Structural Bases for the Antigenicity of VP2 of Infectious Bursal Disease Virus[▽]

Tobias Letzel,[1]† Fasseli Coulibaly,[2]† Felix A. Rey,[3] Bernard Delmas,[4] Erik Jagt,[5]
Adriaan A. M. W. van Loon,[6] and Egbert Mundt[1]*

*Institute of Molecular Biology, Federal Research Institute for Animal Health, Boddenblick 5a, 17493 Greifswald-Insel Riems,
Germany[1]; Laboratory of Structural Biology, School of Biological Sciences, University of Auckland, Auckland,
New Zealand[2]; Unité de Virologie Structurale and URA 3015 CNRS, Département de Virologie,
Institut Pasteur, 25 rue du Dr. Roux, 75724 Paris Cedex 15,[3] and Unité de Virologie et
Immunologie Moléculaires, UR892-INRA, Domaine de Vilvert, 78350 Jouy-en-Josas,[4]
France; and Intervet International B.V., P.O. Box 30, 5830 AA Boxmeer,[5]
and Nobilon International B.V., Exportstraat 39B, P.O. Box 320,
5830 AH Boxmeer,[6] The Netherlands*

Infectious bursal disease virus (IBDV), a member of the family *Birnaviridae*, is responsible for a highly contagious and economically important disease causing immunosuppression in chickens. IBDV variants isolated in the United States exhibit antigenic drift affecting neutralizing epitopes in the capsid protein VP2. To understand antigenic determinants of the virus, we have used a reverse-genetics approach to introduce selected amino acid changes—individually or in combination—into the VP2 gene of the classical IBDV strain D78. We thus generated a total of 42 mutants with changes in 8 amino acids selected by sequence comparison and their locations on loops P_{BC} and P_{HI} at the tip of the VP2 spikes, as shown by the crystal structure of the virion. The antibody reactivities of the mutants generated were assessed using a panel of five monoclonal antibodies (MAbs). Our results show that a few amino acids of the projecting domain of VP2 control the reactivity pattern. Indeed, the binding of four out of the five MAbs analyzed here is affected by mutations in these loops. Furthermore, their importance is highlighted by the fact that some of the engineered mutants display identical reactivity patterns but have different growth phenotypes. Finally, this analysis shows that a new field strain isolated from a chicken flock in Belgium (Bel-IBDV) represents an IBDV variant with a hitherto unobserved antigenic profile, involving one change (P222S) in the P_{BC} loop. Overall, our data provide important new insights for devising efficient vaccines that protect against circulating IBDV strains.

Infectious bursal disease virus (IBDV) is responsible for the highly contagious and immunosuppressive disease IBD in young chickens (5) and has great importance for the poultry industry because it causes significant losses in the industrial production of chickens.

IBDV belongs to the genus *Avibirnavirus* of the family *Birnaviridae* (8). The genome consists of two segments, A and B, of double-stranded RNA, which are encapsidated within a single-shelled icosahedral particle with a diameter of 65 to 70 nm. The larger segment, A, encodes a polyprotein of approximately 110 kDa that is proteolytically cleaved by the viral protease VP4 (4) to form the viral proteins (VP) VP2, VP3, and VP4 and four structural peptides deriving from the VP2 precursor, pVP2 (7). A second open reading frame preceding and partially overlapping the polyprotein gene (2, 35) encodes VP5, which has been detected both in IBDV-infected chicken embryo cells and in bursal cells of IBDV-infected chickens (22).

Antigenic variation among IBDV strains isolated in the United States was reported 20 years ago (16, 25, 33). So far these so-called variant strains seem to be restricted to North America. Variant strains were able to infect and cause disease in chickens with high levels of maternal antibodies against the older classical serotype 1 IBDV strains (25). Cross-neutralization assays showed a restricted ability of sera of chicken vaccinated with classical IBDV to neutralize variant IBDV (13). Snyder et al. (32, 34) established a panel of monoclonal antibodies (MAbs) (e.g., MAbs 10, 57, R63, and B69) for differentiation between several subtypes of IBDV variant strains (e.g., GLS and E/Del) and classical strains (e.g., D78). Together with MAb 67 (36), these antibodies are currently in use for analyses of IBDV field isolates by antigen capture enzyme-linked immunosorbent assay (AC-ELISA) (38). Furthermore, an additional variant strain (variant A), different from GLS and E/Del, was isolated (26). Also, serotype I IBDV was identified in the mid-1980s as evolving in Europe; it exhibited a very virulent phenotype in chickens but was antigenically indistinguishable from the known classical serotype I IBDV (37).

Protein VP2 (441 amino acids [aa]) is the unique component of the icosahedral capsid (6, 29) and the only viral protein recognized by neutralizing antibodies (1, 3, 10). The X-ray structure of VP2 revealed that it is folded into three distinct domains, designated base (B), shell (S), and projection (P) (6,

---

11, 19). The B and S domains are formed by the conserved N- and C-terminal stretches of VP2. In contrast, the P domain consists of the variable region of VP2 (aa 206 to 350) previously identified (2). The antigenic hydrophilic regions A (aa 212 to 224) and B (aa 314 to 325) defined by Azad et al. (1) were found to constitute loops P_{BC} and P_{HI}, respectively, at the outmost part of domain P (see Fig. 3). Deletion studies indicated that the hydrophilic regions A and B may be part of epitopes defined by neutralizing MAbs (1). Amino acid sequence comparison of a variant strain (E/Del) and the Australian strain 002-73 also showed that the reactivities of the MAbs to the different strains were associated with changes in these two loops of VP2 (12). An additional study using several variant (e.g., GLS and E/Del) and classical (e.g., D78 and PBG98) strains, characterized by their reactivities against the MAb panel mentioned above, also suggested the importance of several amino acids of these two loops in antigenic variation (36). In addition, sequence analyses of neutralizing MAb escape mutants showed that loops P_{BC} and P_{HI} are critical for virus neutralization (30). Furthermore, the two additional loops at the top of domain P, loops P_{DE} and P_{FG}, contain aa 253 and 284, respectively, which play important roles in virus infectivity in cell culture (20, 21) and pathogenicity in chickens (39).

In this study, we started from the observation that a new European isolate of IBDV (Bel-IBDV) exhibited a new antigenicity pattern in its reactivity against a MAb panel. We investigated the amino acid differences in the variable region of VP2 in a multiple sequence alignment in order to identify the putative amino acids responsible for the antigenic profile. We then used reverse genetics to introduce selected mutations into the backbone of the classic strain D78 so as to understand the roles of the individual amino acids. We show that the antigenic pattern is controlled by a few amino acids located in two exposed loops (P_{HI} and P_{BC}) of the P domain of VP2.

MATERIALS AND METHODS

Cells. Transfection experiments were performed on baby hamster kidney cells (BHK-21; Collection of Cell Lines in Veterinary Medicine [CCLV], Insel Riems, Germany; RIE 194). Transfection supernatants were passaged on quail muscle (QM) cells (CCLV, Insel Riems, Germany; RIE 466). Chicken embryo cells derived from embryonated specific-pathogen-free (SPF) eggs (Valo; Lohmann, Cuxhaven, Germany) were used for establishment of growth kinetics. Cells were cultivated in medium 199 supplemented with 10% fetal calf serum, in the presence of penicillin (100 IU/ml) and streptomycin (100 μg/ml).

Virus. Progeny from a chicken flock in Belgium vaccinated with a classical vaccine showed wet litter, general immunosuppression, and low weight gain but low mortality (1 to 2%). Chickens from this flock were examined postmortem. The bursae fabricii (BF) of affected chickens were collected, homogenized, and tested by AC-ELISA (38) using MAbs 57, R63, 67, B69, and 10. As a control and for comparison, two virus isolates from variant strains isolated in the mid-1980s in the United States, such as E/Del (26) or GLS (34), and one classical strain, D78 (Nobilis Gumboro D78; Intervet, Boxmeer, The Netherlands), were used in the AC-ELISA. BF material that showed an altered AC-ELISA reactivity pattern compared to that of the IBDV strains used was passaged in chickens. A BF homogenate was administered to 14-day-old SPF chickens (Intervet, Boxmeer, The Netherlands) housed in negative-pressure-filtered air isolators. Four days after inoculation, the presence of IBDV in the BF was investigated using the MAbs in the AC-ELISA, and IBDVs with the altered reactivity pattern were used for further investigations. The isolate was termed Bel-IBDV.

Amplification and analysis of the Bel-IBDV isolate. Homogenized bursal tissue of SPF chickens infected with Bel-IBDV was incubated with proteinase K (0.5 mg/ml)–sodium dodecyl sulfate (0.5%) overnight at 37°C. After purification of RNA, the VP2 part of the polyprotein gene was obtained by reverse transcription-

PCR (RT-PCR) essentially as described elsewhere (23). Three fragments, BelgF1, BelgF2, and BelgF3, were amplified by primer pairs IBDVFP1–IBDVRP1, IBDVFP2–IBDVRP2, and IBDVFP3–IBDVRP3, respectively (available from author upon request). After blunt-end ligation into SmaI-cleaved pUC18 (Pharmacia), three different plasmids were obtained (pUC18BelgF1, pUC18BelgF2, and pUC18BelgF3). Three independent plasmids each were sequenced, and a consensus sequence was determined. Fragments containing the consensus sequence were combined by ligation using appropriate overlapping restriction enzyme cleavage sites to obtain pUC18Belg123 (see Fig. 1). This plasmid was cleaved by EcoRI/SacII, and the Bel-IBDV fragment containing nucleotides 1 to 1760 (numbering in accordance with reference 23) was ligated into the appropriately cleaved pD78A to obtain pD78A-Belg.

In order to assay the reactivities of E/Del and GLS sequences, recombinant plasmids were generated using pD78A as a backbone. To this end, bursa materials of chickens infected with either E/Del or GLS were treated as described above. RT-PCRs were performed using oligonucleotides IBDVFP1–IBDVRP3 (available from author upon request), and the PCR fragments were cloned after EcoRI/SacII digestion into appropriately cleaved pD78A. The plasmids obtained (pD78A-E/Del and pD78A-GLS) were sequenced and used for subsequent analysis. A schematic drawing of the plasmids is shown in Fig. 1.

Generation of mutated segment A. For site-directed mutagenesis, pD78A (24) was cleaved with EcoRI/KpnI, and the segment A-containing fragment was ligated into appropriately cleaved pBlueScript KS(+) to obtain pSK+-D78A. After preparation of single-stranded DNA (ssDNA) (18), site-directed mutagenesis was performed according to the procedure of Kunkel et al. (18) using oligonucleotides as specified (available from author upon request). Oligonucleotides Mut1, Mut2, Mut3, Mut4, Mut5, Mut6, Mut7, Mut8, Mut9, Mut10, and Mut11 were used to generate the respective mutated plasmids pMut1 to pMut11. Additional site-directed mutagenesis experiments were performed using ssDNA resulting from the mutated plasmids or pSK+-D78A and oligonucleotide P222S, P222T, or R330S (available from author upon request). Experiments were performed with either one mutagenic oligonucleotide, to obtain plasmids with an additional mutation of aa 222 (proline to threonine or serine) or 330 (arginine to serine), or with two oligonucleotides in parallel, resulting in two amino acid substitutions (P222S and R330S) in one plasmid. The resulting plasmids (Table 1) were sequenced and used for further experiments.

For site-directed mutagenesis of Bel-IBDV VP2, plasmid pD78A-Belg was cleaved with EcoRI/KpnI and cloned into appropriately cleaved pSK+. The ssDNA of plasmid pSK+D78-Belg that was obtained was used for site-directed mutagenesis using oligonucleotide S222P (available from author upon request) to change aa 222 from serine to proline. The resulting plasmid, pSK+-D78A-BelgS222P, was sequenced and used for further experiments.

Transfection of cRNA, immunofluorescence assays, and passaging of generated virus. For in vitro transcription, plasmids pD78A, pD78A-E/Del, pD78A-GLS, and pD78A-Belg and derivatives of pD78A were linearized by cleavage with BsrGI. pP2B (24) was linearized using PstI. Further treatment of linearized DNA, transcription, and transfection of RNA into BHK-21 cells were carried out as described elsewhere (21). For immunofluorescence assays, BHK-21 cells grown on coverslips in six-well tissue culture plates were transfected, fixed 24 h later with ice-cold ethanol for 5 min, and air dried. Fixed cells were incubated for 30 min with MAb 57, R63, 67, B69, or 10 diluted in phosphate-buffered saline and were processed for immunofluorescence using dichlorotriazinylaminofluorescein (DTAF)-conjugated goat anti-mouse immunoglobulin G. The cells were investigated by confocal laser scan microscopy using an LFM510 (Zeiss, Göttingen, Germany).

For virus propagation, transfected BHK-21 cells were frozen and thawed once, and the supernatant obtained after centrifugation was passaged in QM-cells until a cytopathic effect (CPE) was visible. The supernatant was obtained as described above, aliquoted, and stored at −70°C. For analysis of viability and reactivity with MAbs, QM cells grown in 24-well tissue culture plates were infected with one aliquot, incubated for 24 h, and processed for immunofluorescence.

Growth analysis of recombinant virus in cell culture. To monitor virus replication, chicken embryo cells grown in 24-well tissue culture plates were infected with selected IBDV at a multiplicity of infection of 1 for 1 h at 37°C. After removal of the inoculum, cells were washed with serum-free medium, and 1 ml medium was added. Supernatants were harvested separately either immediately thereafter (0 h) or after 8, 16, 24, 36, or 48 h of incubation at 37°C and were stored at −70°C. Virus titers were determined as 50% tissue culture infective doses ($TCID_{50}$) by using QM cells grown in 96-well tissue culture plates according to standard procedures. Five days later, wells exhibiting CPE were counted as positive, and the virus titer ($TCID_{50}$) was determined (17). Average values and standard deviations for three independent experiments were calculated. The

TABLE 1. Results of cotransfection experiments of cRNA with different segment A's and pP2B's

Plasmid[a]	Amino acid[b] at position:					Result with MAb[c]:				
	222	318	321	323	330	57	R63	67	B69	10
pD78A	P	G	A	D	R	−	+	−	+	+
pD78A-R330S	P	G	A	D	S	−	+	−	+	+
pD78A-E/Del	T	D	A	E	S	−	+	+	−	−
pD78A-GLS	T	G	E	D	S	+	−	−	−	+
pD78A-P222S	S	G	A	D	R	−	+	+	+	+
pD78A-P222T	T	G	A	D	R	−	+	+	+	+
pD78-P222S-R330S	S	G	A	D	S	−	+	+	+	+
pMut1	P	D	A	D	R	−	+	−	+	−
pMut1-R330S	P	D	A	D	S	−	+	−	+	−
pMut2	P	D	A	E	R	−	+	−	+	−
pMut2-R330S	P	D	A	E	S	−	+	−	+	−
pMut3-R330S	P	D	E	D	S	−	+	−	+	−
pMut5	P	G	A	E	R	−	+	−	+	−
pMut5-R330S	P	G	A	E	S	−	+	−	+	−
pMut8	P	N	A	D	R	−	+	−	+	−
pMut8-P222S	S	N	A	D	R	−	+	−	+	−
pMut8-R330S	P	N	A	D	S	−	+	−	+	−
pMut9	P	N	A	E	R	−	+	−	+	−
pMut9-R330S	P	N	A	E	S	−	+	−	+	−
pMut10-R330S	P	N	E	D	S	−	+	−	+	−
pMut11-R330S	P	N	E	E	S	−	+	−	+	−
pMut1-P222S	S	D	A	D	R	−	+	+	+	−
pMut1-P222S-R330S	S	D	A	D	S	−	+	+	+	−
pMut2-P222S	S	D	A	E	R	−	+	+	+	−
pMut2-P222T	T	D	A	E	R	−	+	+	+	−
pMut2-P222S-R330S	S	D	A	E	S	−	+	+	+	−
pMut5-P222S	S	G	A	E	R	−	+	+	+	−
pMut5-P222T	T	G	A	E	R	−	+	+	+	−
pMut9-P222S	S	N	A	E	R	−	+	+	+	−
pMut9-P222T	T	N	A	E	R	−	+	+	+	−
pMut3	P	D	E	D	R	+	−	−	+	−
pMut3-P222S	S	D	E	D	R	+	−	−	+	−
pMut10	P	N	E	D	R	+	−	−	+	−
pMut10-P222S	S	N	E	D	R	+	−	−	+	−
pMut11	P	N	E	E	R	+	−	−	+	−
pMut11-P222S	S	N	E	E	R	+	−	−	+	−
pMut6	P	G	E	D	R	+	−	−	+	+
pMut6-P222S	S	G	E	D	R	+	−	−	+	+
pMut6-R330S	P	G	E	D	S	+	−	−	+	+
pMut4	P	D	E	E	R	−	−	−	+	−
pMut4-P222S	S	D	E	E	R	−	−	−	+	−
pMut4-R330S	P	D	E	E	S	−	−	−	+	−
pMut7	P	G	E	E	R	−	−	−	+	−
pMut7-P222S	S	G	E	E	R	−	−	−	+	−
pMut7-R330S	P	G	E	E	S	−	−	−	+	−

[a] Plasmids were used for transfection experiments.
[b] Amino acids changed by site-directed mutagenesis are boldfaced.
[c] MAbs were used for immunofluorescence assays.

diluted virus suspensions used for infection were titrated after dilution for confirmation of the titer used for infection.

Characterization of virus mutants by neutralization assay. Neutralization assays were performed as described previously (31) using QM cells. Cells were seeded at a density of 10^6/ml. The end point of the virus neutralization test for a serum sample was defined as the reciprocal value of the highest dilution (log_2) of the antibodies at which no CPE was visible.

Structural models of VP2 mutants. To gain further insights into the requirements for recognition of VP2 by MAbs 57 and 67, the mutations affecting their binding were modeled on the background of the recently published X-ray structure of VP2 from IBDV strain CT (6) with the Modeler program (28). The loops analyzed in this study were poorly defined in the structure at 3 Å with high-temperature factors and some side chain density missing; thus, caution was exercised in describing atomic interactions. Illustrations were prepared with PyMol (W. L. DeLano, The PyMOL Molecular Graphics System, 2002; DeLano Scientific, San Carlos, CA).

RESULTS

Identification of a European IBDV variant strain. Bel-IBDV was first analyzed by AC-ELISA in comparison with the classical strain D78 and the variant strains E/Del and GLS (Table 2) by using bursa materials of infected chickens and the MAbs described above. The reactivity patterns for the classical strain D78 and the two variant strains (GLS, E/Del) were as expected and previously described (36). Interestingly, Bel-IBDV displayed a unique pattern, suggesting that the isolated virus was a new, to date unknown antigenic IBDV variant strain. To confirm these data and to establish the tools for a detailed analysis of the antigenic determinants, pD78A deriv-
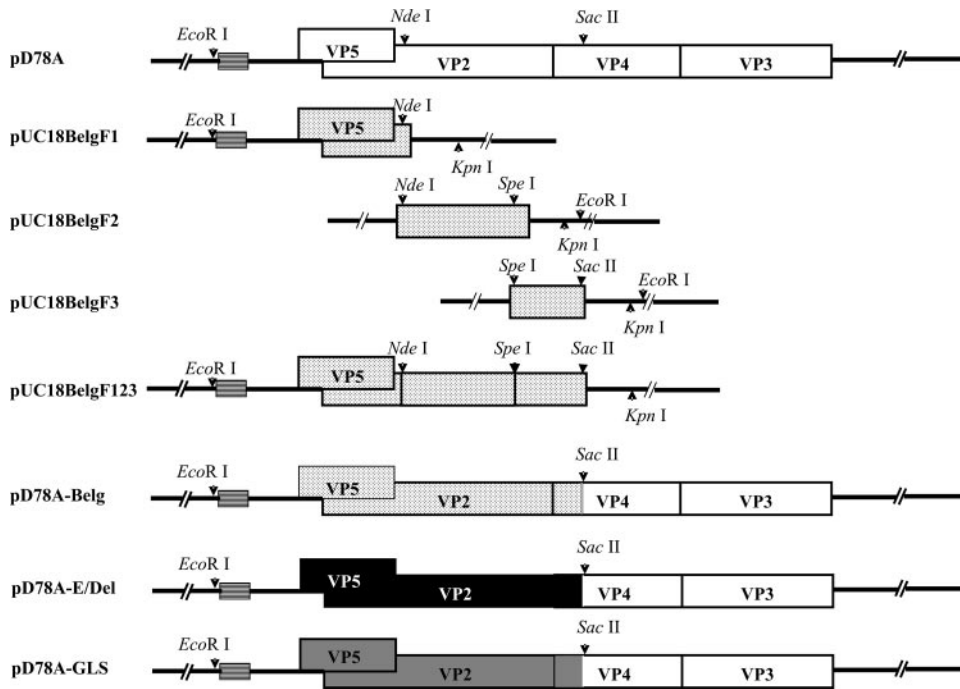
FIG. 1. Construction of a chimeric cDNA clone of segment A of IBDV. The genomic organization of IBDV segment A is shown at the top. Open rectangles, coding sequences of segment A of strain D78; stippled rectangles, sequences of the Belgian (Belg) isolate; solid rectangles, E/Del sequences; dark shaded rectangles, GLS sequences; horizontally striped boxes, the T7 promoter. Arrowheads mark the locations of restriction enzyme sites used during cloning, and the restriction enzymes are given.

ative plasmids encoding VP2 proteins of different strains were constructed (Fig. 1) and transfected into cells. Immunofluorescence analysis confirmed the AC-ELISA results: each full-length pD78A derivative encoding a certain VP2 (D78, GLS, E/Del, Bel-IBDV) displayed a unique pattern identical to that obtained with the parental viruses in the AC-ELISA (Fig. 2). Thus, this MAb collection allows for differentiation of antigenic patterns, each of which is representative of one of the strains used in the study.

Amino acid sequence analysis of the variable region of VP2. To understand the relative importance of residues of the P domain (the variable region of VP2) in the modulation of VP2 antigenicity, the amino acid sequences of the P domains of strains D78, E/Del, GLS, and Bel-IBDV and isolate GA198 (15) were first aligned (Fig. 3A). GA198 was chosen after a GenBank search due to its unusual amino acid composition in the P_{HI} loop, where an asparagine was present at amino acid position 318. Since amino acids located in two of the loops in

the P domain (P_{BC} and P_{HI}) have been proposed to influence the formation of neutralizing epitopes (1), these two immunodominant loops were analyzed in detail. Amino acid differences were observed in loop P_{BC} at a single position (P222T and P222S) and in loop P_{HI} at three positions (G318D, G318N, A321E, and D323E). The amino acid sequence of Bel-IBDV

TABLE 2. Reactivities of different IBDV strains by AC-ELISA in comparison to Bel-IBDV

Virus[a]	Result with MAb[b]:				
	57	R63	67	B69	10
Bel-IBDV	−	+	+	+	+
E/Del	−	+	+	−	−
GLS	+	−	−	−	+
D78	−	+	−	+	+

[a] Virus used as the antigen in the ELISA.
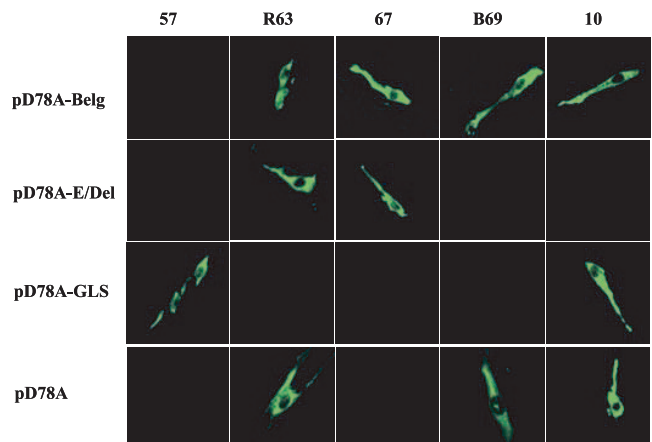[b] MAbs (57, R63, 67, B69, 10) used for the immunofluorescence assay.

FIG. 2. Immunofluorescence after transfection of cRNA of segment A. BHK-21 cells were cotransfected with in vitro-transcribed capped cRNAs from cDNA plasmids containing either the full-length sequences (pD78A) or a chimeric segment A (pD78-Belg, pD78A-GLS, pD78A-E/Del) and cRNA of pP2B. Acetone-fixed cells were incubated with MAbs 10, 57, R63, 67, and B69 against the viral protein VP2. The reactivities of the MAbs were detected by DTAF-conjugated goat anti-mouse antibodies.
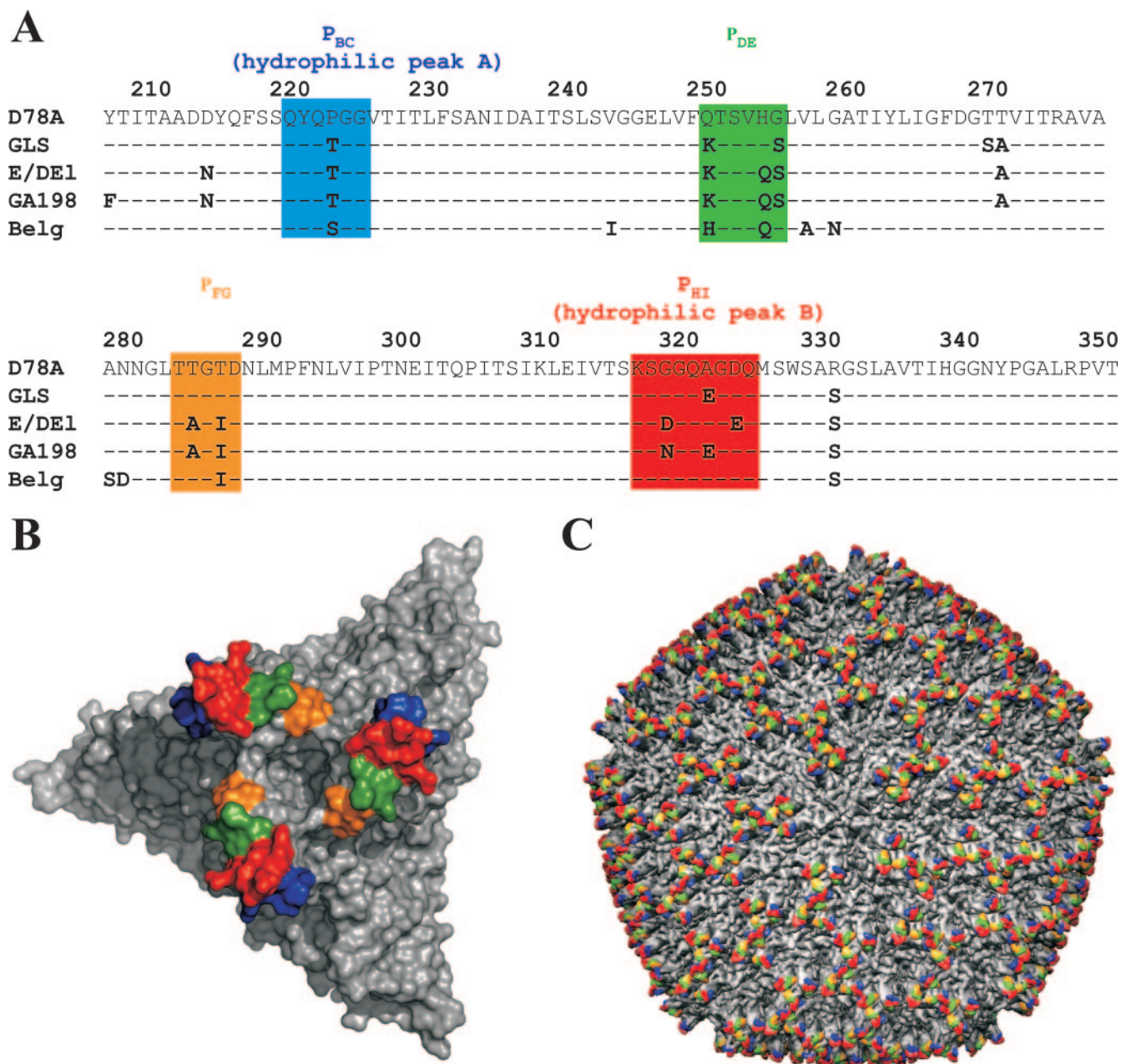
FIG. 3. Comparison of the amino acid sequences of the variable region of IBDV segment A. (A) Amino acid sequences (aa 206 to 350) of IBDV strains D78, GLS, and E/Del, the Belgian isolate, and isolate GA198 (aa 216 to 350) were compared. The sequences of D78, GLS, and E/Del were taken from the report of Vakharia et al. (36). The sequence of isolate GA198 was taken from GenBank (accession no. AAV48814). The sequence of the Belgian isolate was established in this study. The two hydrophilic peaks A and B, as described previously (1), are shown (see the text). Loops P_{BC}, P_{DE}, P_{FG}, and P_{HI} of domain P of VP2 (6) are boxed in the sequence alignment in blue, green, yellow, and red, respectively. Amino acid sequences are numbered in accordance with the work of Mundt and Müller (23). (B) Surface representation of the trimer, with each surface loop of domain P colored according to the alignment presented in panel A. (C) Locations of the trimers and antigenic loops in the overall structure of the virus particle.

revealed one specific amino acid change (P222S) in the P_{BC} loop. These observations suggest that a few residues control VP2 antigenicity. The locations of the single loops described above are depicted on the surface of a single VP2 trimer (Fig. 3B) and on the whole virus capsid (Fig. 3C). This illustrates the importance of the four hydrophilic loops, propagated 780

times by the T=13 icosahedral symmetry of the virion, with the likely ability to bind neutralizing antibodies.

The identification of several residues in loops P_{BC} and P_{HI} associated with antigenic variability prompted us to analyze how single and multiple substitutions in these loops can modulate antibody binding. This study was focused on the amino
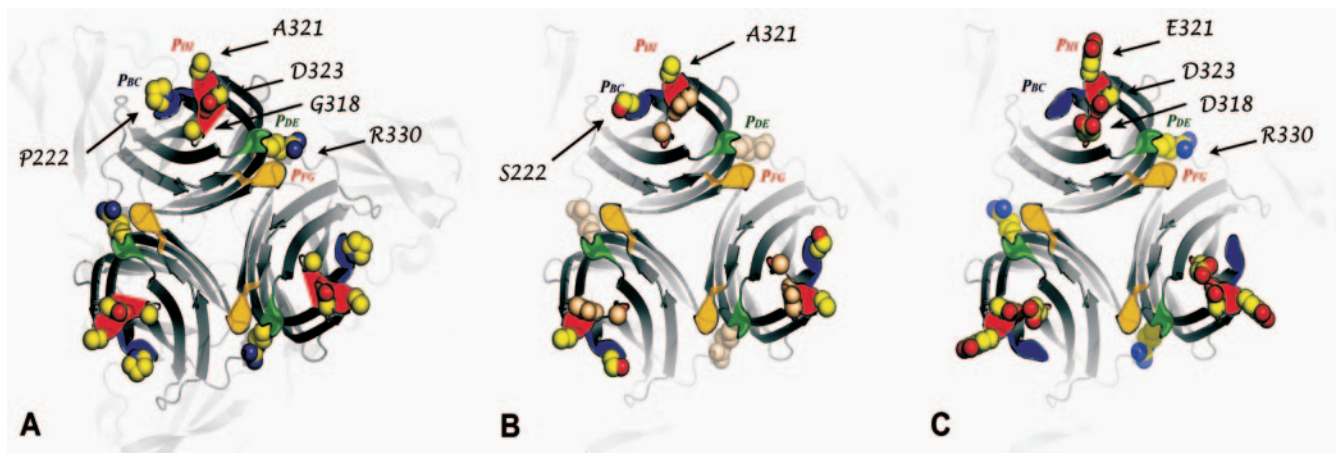
FIG. 4. Structural modeling of amino acid changes influencing the binding of MAbs 57 and 67. Exposed loops from domain P are highlighted with the same color scheme as that for Fig. 3 on a cartoon representation of the VP2 trimer. (A) Side chains of all amino acids involved in this study of IBDV strain D78 are represented as spheres. (B and C) Residues involved in the recognition of VP2 by MAbs 67 and 57 are highlighted on a model of D78-P222S (B) and Mut3 (C), respectively.

acids determining the binding of MAbs 57, R63, 67, B69, and 10. It should be noted that all these epitopes were present only during experiments using immunofluorescence (Fig. 2) and immunoprecipitation (data not shown). The lack of reactivity in Western blot experiments (data not shown) suggests that they are confirmation dependent. Structural models of selected VP2 forms (D78, D78-PS, Mut3) with different MAb binding patterns are shown in Fig. 4.

Single and multiple amino acid substitutions in both loops P_{BC} and P_{HI} of VP2 control reactivity to MAbs. Substitutions at positions 222, 318, 321, and 323, either singly or in combination, were engineered on the D78 segment A backbone to identify residues associated with the different antigenic patterns (Table 2). Substitution of aa 330 was also included due to the presence of serine at this position in all IBDV strains compared except for strain D78. Immunoreactivity was analyzed by indirect immunofluorescence after cotransfection of a pD78A derivative with pP2B cRNA.

(i) MAb 67 epitope. The reactivity of the MAb 67 epitope involves specific amino acids in the two loops P_{BC} and P_{HI}. The presence of both a serine/threonine at position 222 (P_{BC} loop) and an alanine at position 321 (P_{HI} loop) is necessary for the recognition of this epitope, showing that this epitope is defined by amino acids that are 100 residues apart on the VP2 primary sequence. Substitutions at positions 318, 323, and 330 had no effects on the binding of MAb 67.

The critical role of positions 222 and 321 for recognition by MAb 67 is illustrated with D78-PS in Fig. 4B. Although these residues are distant in the VP2 primary sequence, they are located in loops P_{BC} and P_{HI}, respectively, which are in close proximity at the tip of VP2 spike. The amino acid at position 222 is exposed to a solvent and could therefore interact directly with MAb 67. As a consequence, serine or threonine at position 222 is likely to be part of the epitope. On the other hand, alanine 321 is unlikely to be a critical part of the epitope, and loss of recognition by MAb 67 with a glutamate at position 321 probably results from the masking of surrounding residues of loop P_{HI} as observed by computer modeling (data not shown).

(ii) MAb 57 epitope. Recognition of the MAb 57 epitope involves the P_{HI} loop and a particular residue in position 330 but not the P_{BC} loop. A glutamic acid at position 321 located in the P_{HI} loop is a requisite for the binding of MAb 57 to this epitope (Table 1), as shown for Mut3 in Fig. 4C. An aspartic acid at position 323, instead of a glutamic acid, also contributes to the binding of MAb 57. With one notable exception (pMut11 and one of its derivatives), a glutamic acid at position 323 correlated with binding of MAb 57. For pMut11, asparagine at position 318, instead of glycine or glutamic acid at position 321, appears to compensate for the lack of aspartic acid at position 323 (see the difference in reactivity between pMut7 and pMut11 [Table 1]). In addition, serine 330 is generally not tolerated, with some notable exceptions: pMut6-R330S was recognized by MAb 57. Thus, the reactivity of the MAb 57 epitope appears to depend on at least one critical residue, glutamic acid 321, and on two more-dispensable residues, aspartic acid 323 and arginine 330.

While E321 is exposed and could constitute part of the MAb 57 epitope, residues 323 and 330 seem to have an indirect role in altering the backbone of VP2. Modeling analysis suggests that a D323E mutation could break a stabilizing salt bridge with lysine 316 within the P_{HI} loop (data not shown). Further experiments need to be performed to confirm this hypothesis. Residue 330 is located at the interface between subunits in the trimeric spike, away from the main antigenic site formed by loops P_{BC} and P_{HI}. Arginine 330 appears to stabilize a bulge by interaction with glutamates 212 and 213 of the P_B β-strand (data not shown). Thus, it is possible that the R330S mutation leads to subtle alterations in the jelly roll, ultimately leading to a different conformation of loop P_{BC} that is incompatible with the binding of MAb 57.

Finally, these data provide a rationale for understanding why IBDV variants recognized by MAb 67 are not recognized by MAb 57, and vice versa. This restriction is due to a single substitution at position 321 at the tip of the VP2 spike: a glutamic acid at this position allows MAb 57 binding, while an alanine allows MAb 67 binding.

TABLE 3. Neutralization assay of IBDV mutants using a polyclonal serum and MAbs

Virus[a]	Result of IIFA[b] with MAb:					Titer of antibody[c] in neutralization assay					
	57	R63	67	B69	10	57	R63	67	B69	10	Anti-IBDV
rD78	−	+	−	+	+	$<2^d$	>4,096	<2	4,096	2,048	4,096
PS-D78	−	+	+	+	+	<2	>4,096	1,024	2,048	2,048	4,096
Mut1	−	+	−	+	−	<2	>4,096	<2	1,024	<2	256
PS-Mut1	−	+	+	+	−	<2	>4,096	2,048	1,024	<2	1,024
Mut2	−	+	−	+	−	<2	>4,096	<2	2,048	<2	512
PS-Mut2	−	+	+	+	−	<2	4,096	4096	1,024	<2	128
Mut10	+	−	−	+	−	2048	<2	<2	1,024	<2	512
Mut11	+	−	−	+	−	<2	<2	<2	4,096	<2	256
D78-Belg	−	+	+	+	+	<2	<2	2048	4,096	2,048	256
D78-BelgS222P	−	+	−	+	+	<2	<2	<2	4,096	1,024	256

[a] Recombinant IBDV used in the neutralization assay.
[b] IIFA, indirect immunofluorescence assay.
[c] Reciprocal value of the highest dilution ($\log_2$) of the antibodies in which no CPE was visible. Five MAbs (57, R63, 67, B69, 10) and one polyclonal rabbit anti-IBDV serum were used in the neutralization assay.

(iii) **MAb R63 epitope.** When an alanine is present at position 321, there is always reactivity with MAb R63, showing that loop P_{HI} controls the binding of this MAb. However, alanine at position 321 is not an absolute requirement for reactivity. Depending on adequate substitution at some other positions, even the presence of alanine 321 is dispensable (see data for pMut10-R330S and pMut11-R330S constructs in Table 1). Thus, the reactivity of MAb R63 appears to be less restricted than that of MAb 67, which requires an alanine at position 321 and a serine or threonine at position 222, as described above.

(iv) **MAb 10 epitope.** Two residues appear to be critical for the presence of the MAb 10 epitope: glycine at position 318 and aspartic acid at position 323. The reactivity of MAb 10 was not influenced by any of the substitutions carried out at other positions (positions 222, 321, and 330).

(v) **MAb B69 epitope.** None of the substitutions carried out on the pD78A backbone at positions 222, 318, 321, 323, and 330 altered the reactivity of the MAb B69 epitope, suggesting that neither the P_{BC} nor the P_{HI} loop is involved. To determine if a third loop (P_{DE} loop [Fig. 3]) present at the top of the VP2 projection could contribute to this epitope, a series of additional single or multiple substitutions were engineered in the pD78A backbone at positions 249, 254, and 270. None of the single (Q249K, G254S, or T270A) or combined (Q249K G254S, Q249K T270A, or Q249K G254S T270A) substitutions were able to alter the epitope defined by MAb B69, indicating that this third loop probably is not associated with the presence of this epitope (data not shown).

(vi) **The unique antigenic pattern of IBDV-Belg.** The results obtained also suggested that the reactivity of IBDV-Belg with MAb 67 was caused by a single substitution at position 222 (P222S). To provide additional evidence that the serine in position 222 is critical for MAb 67 binding, this position was mutated in the IBDV-Belg VP2 backbone. Thus, a plasmid (pD78A-Belg) coding for segment A and containing the complete VP2 gene segment of the Belgian isolate mutated at position 222 (S222P) was constructed. While VP2 encoded by pD78A-Belg was reactive with MAb 67, the corresponding S222P mutant was not (Table 3).

Analysis of the immunoreactivity of the corresponding recombinant viruses by a neutralization assay. Ten different cDNAs encoding VP2 mutants with unique antigenic and/or

sequence patterns were chosen to produce mutants by reverse genetics and to confirm by a neutralization assay the importance of the P_{BC} and P_{HI} loops in VP2 antigenicity. Virus mutants were produced as described in Materials and Methods, and their ability to be neutralized by each MAb was measured (Table 3). In most cases, when a virus mutant was recognized by a MAb in the immunofluorescence assay, it was efficiently neutralized by the same MAb. One exception was observed with Mut11, which was recognized in the immunofluorescence assay by MAb 57 but was not neutralized. The fact that Mut10, which differs from Mut11 by a single substitution at position 323, was neutralized by MAb 57 suggests that the aspartic acid at position 323 contributes to the reactivity of this epitope. Confirmation of the relative importance of position 222 in MAb 67 binding was provided by this neutralization assay using D78-Belg and D78-BelgS222P.

Analysis of growth in cell culture. To test whether the amino acid substitutions influenced the replication of mutated viruses in cell culture, several IBDV mutants generated by reverse genetics were analyzed in comparison to the recombinant D78 virus (Fig. 5). Mutation of aa 222 from proline to serine did not influence replication in cell culture. In contrast, all amino acid changes in the P_{HI} loop influenced the replication of the corresponding mutants. These mutants grew to lower titers at all time points investigated, indicating that the three residues of the P_{HI} loop in positions 318, 321, and 323 are important parameters for replication in cell culture.

To exclude the possibility that the virus used for the growth curve and the neutralization assays exhibited revertant mutations, RT-PCRs using the IBDVFP1–IBDVRP3 primer pair (available from author upon request) and Deep Vent polymerase (New England Biolabs) were carried out on the propagated viruses. Sequence analysis of cloned PCR products revealed either no mutations or only silent mutations.

DISCUSSION

Since the 1980s, IBDV strains that are able to overcome the protection induced by the attenuated serotype I IBDV vaccines have been isolated regularly (25). Compared to the IBDV strains isolated before 1985, these new variant strains showed particular antigenic profiles (25, 26, 27, 33, 34, 36). To
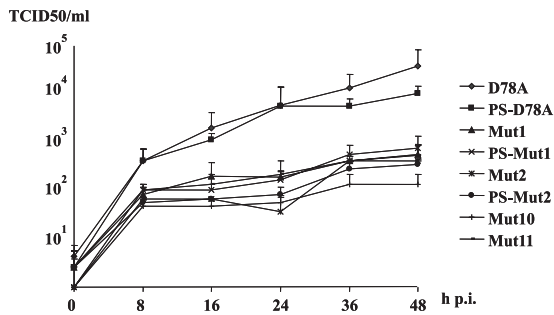
TCID50/ml

FIG. 5. Replication kinetics of recombinant IBDV in cell culture. Embryonic chicken cells were infected with IBDV D78, PS-D78, Mut1, PS-Mut1, Mut2, PS-Mut2, Mut10, or Mut11 as described in Materials and Methods. Supernatants removed at the indicated times (hours) postinfection (h p.i.) were used for determination of viral titers, expressed in $TCID_{50}$ per milliliter. Values were plotted logarithmically on the vertical axis. Average titers and standard deviations (error bars) from three independent experiments are shown.

identify the amino acids of VP2 responsible for reactivity with neutralizing antibodies in more detail, we used a reverse-genetics approach (24) with the segment A-encoding hybrid constructs of VP2. This method has the advantage of allowing the analysis of antigenic determinants of IBDV strains that are unable to infect cells in vitro.

In this study, we showed that a few residues of VP2 contribute substantially to the antigenic properties of IBDV. In fact, we found that only five residues located in two structural loops (P_{BC} and P_{HI}) at the tip of the VP2 P domain deeply modulate its immunoreactivity. The atomic models that we built, modeling the mutations on the crystal structure of the IBDV particle, suggested that substitutions of amino acids at the tip of the VP2 P domain do not result in destabilization of the overall folding of VP2. This indicates that MAb binding is controlled by small changes at the surface of VP2. Our study has established several additional features: (i) while the presence of a specific residue can be necessary for the recognition of an epitope, other residues can contribute less critically to its reactivity (for instance, alanine at position 321 is required for MAb 57 binding, but the presence of an aspartic acid at position 323 appears only to facilitate the recognition of the epitope); (ii) amino acids modulating the binding of MAbs 57 and 67 are adjacent in the 3-dimensional structure of VP2, although they are distant in sequence; (iii) in some cases, the reactivity of an epitope excludes the binding of another antibody (see the reactivity patterns of MAbs 57 and R63 in Table 1). In addition, during this study, the binding of MAb B69 was not influenced by any of the amino acid substitutions engineered. Vakharia et al. (36) hypothesized that glutamine at position 249 could be critical for the binding of MAb B69. The ability of Bel-IBDV to bind MAb B69 with a histidine at this position suggests that several amino acids at position 249 can accommodate MAb B69 reactivity (Fig. 2). It is likely that B69 binds at a different region of VP2, away from both loops (P_{BC} and P_{HI}): Snyder et al. (32) showed by binding studies using a competitive ELISA that two epitopes (R63 and B69) were not overlapping. Figure 3C shows extended regions of the IBDV particle surface, around the icosahedral fivefold and quasi-sixfold axes of the T=13 lattice, that are away from domain P,

suggesting that MAb B69 could very well bind to the S domain of VP2.

Using an IBDV reverse-genetic system, we also observed that replication of several IBDV recombinants was impaired relative to that of the recombinant D78 strain. All IBDV strains containing amino acid substitutions in loop P_{HI} grew to significantly lower titers than the parental strain D78. In contrast, mutation of aa 222 (Pro to Ser) in loop P_{BC} showed no significant influence on replication in cell culture. It is possible that substitutions in loop P_{HI} result in a lower efficiency of viral particle assembly either by altering VP2 folding or by destabilizing the virion. However, the crystal structure of VP2 indicates that the locations of these residues, pointing toward the outside of the molecule, are not likely to affect the 3-dimensional fold when their side chains are mutated.

Alternatively, these changes in loop P_{HI} may influence the ability of VP2 to bind to IBDV cellular receptors. The location of loop P_{HI}—adjacent to loop P_{DE}, which modulates the adaptation of the virus to cell culture and is involved in particle-particle interaction (11)—supports the latter hypothesis.

Interestingly, two of the IBDV mutants produced in this study were recognized by a neutralizing MAb but were not neutralized identically. Both mutants (Mut10 and Mut11) were recognized by MAb 57, but only Mut10 was neutralized. Thus, the only substitution differentiating Mut10 and Mut11—D323E, located in loop P_{HI}—results in different functional properties of MAb 57. It can be hypothesized that the amino acid change resulted in a lower binding affinity of MAb 57 for VP2 that was not sufficient for neutralization of the virus. Binding affinity studies with the different mutants should clarify this issue.

We also characterized a new European isolate from Belgium (Bel-IBDV) that showed a unique reactivity pattern characterized by recognition of MAbs B69, R63, 10, and 67, a hitherto unseen combination. This indicated that mutations occurred within circulating European strains or that a new virus has been introduced into European chicken populations. A third option is that this virus has been circulating undetected for decades. This seems plausible, since Domanska et al. (9) described sequences of IBDV strains present during the late 1970s and early 1980s in Europe containing a serine at position 222 and causing subclinical infectious bursal disease. Interestingly, Jackwood et al. (14) recently reported the presence of new IBDV isolates in Europe with VP2 sequences distinct from those of previous European IBDV isolates (classical and very virulent) and Belg-IBDV. The sequences were highly related to an IBDV variant circulating in the United States. Based on our study, we predict that the reaction pattern is likely to be the same as that of the E/Del variant strains, due to the presence of serine or threonine at position 222, aspartic acid at 318, and glutamatic acid at 323.

In summary, our study shows that distinct amino acids located in loops P_{BC} and P_{HI} of VP2 strongly influence the reactivities of neutralizing epitopes by different mechanisms. This knowledge will be very useful for the design of new tailored IBDV vaccines with broad-spectrum efficacy. We also detected the presence of an IBDV strain with a unique antigenic profile in Europe. Two questions remain open: does this strain represent a new type of antigenic variant that will spread in Europe? are the vaccines used currently able to protect

against this new subtype of IBDV? Further analyses like the one presented here are likely to provide answers to these important questions.

REFERENCES

1. Azad, A. A., M. N. Jagadish, M. A. Brown, and P. J. Hudson. 1987. Deletions mapping and expression in *Escherichia coli* of the large genomic segment of a birnavirus. Virology 161:145–152.

2. Bayliss, C. D., U. Spies, K. Shaw, R. W. Peters, A. Papageorgiou, H. Müller, and M. E. G. Boursnell. 1990. A comparison of the sequences of segment A of four infectious bursal disease virus strains and identification of a variable region in VP2. J. Gen. Virol. 71:1303–1312.

3. Becht, H., H. Müller, and H. K. Müller. 1988. Comparative studies on structural and antigenic properties of two serotypes of infectious bursal disease virus. J. Gen. Virol. 69:631–640.

4. Birghan, C., E. Mundt, and A. E. Gorbalenya. 2000. A non-canonical Lon proteinase deficient of the ATPase domain employs the Ser-Lys catalytic dyad to impose broad control over the life cycle of a double-stranded RNA virus. EMBO J. 19:114–123.

5. Cosgrove, A. S. 1962. An apparently new disease of chickens—avian nephrosis. Avian Dis. 6:385–389.

6. Coulibaly, F., C. Chevalier, I. Gutsche, J. Pous, J. Navaza, S. Bressanelli, B. Delmas, and F. A. Rey. 2005. The birnavirus crystal structure reveals structural relationships among icosahedral viruses. Cell 120:761–772.

7. Da Costa, B., C. Chevalier, C. Henry, J. C. Huet, S. Petit, J. Lepault, H. Boot, and B. Delmas. 2002. The capsid of infectious bursal disease virus contains several small peptides arising from the maturation process of pVP2. J. Virol. 76:2393–2402.

8. Delmas, B., F. S. B. Kibenge, J. C. Leong, E. Mundt, V. N. Vakharia, and J. L. Wu. 2005. *Birnaviridae*, p. 561–569. *In* C. M. Fauquet, M. A. Mayo, J. Maniloff, U. Desselberger, and L. A. Ball (ed.), Virus taxonomy. VIIIth report of the International Committee on Taxonomy of Viruses. Elsevier/Academic Press, London, United Kingdom.

9. Domanska, K., T. Mato, G. Rivallan, K. Smietanka, Z. Minta, C. de Boisseson, D. Toquin, B. Lomniczi, V. Palya, and N. Eterradossi. 2004. Antigenic and genetic diversity of early European isolates of infectious bursal disease virus prior to the emergence of the very virulent viruses: early European epidemiology of infectious bursal disease virus revisited? Arch. Virol. 149:465–480.

10. Fahey, K. J., K. Erny, and J. Crooks. 1989. A conformational immunogen on VP2 of infectious bursal disease virus that induces virus-neutralizing antibodies that passively protect chickens. J. Gen. Virol. 70:1473–1481.

11. Garriga, D., J. Querol-Audi, F. Abaitua, I. Saugar, J. Pous, N. Verdaguer, J. R. Caston, and J. F. Rodriguez. 2006. The 2.6-Angstrom structure of infectious bursal disease virus-derived T=1 particles reveals new stabilizing elements of the virus capsid. J. Virol. 80:6895–6905.

12. Heine, H. G., M. Haritou, P. Failla, K. Fahey, and A. Azad. 1991. Sequence analysis and expression of the host-protective immunogen VP2 of a variant strain of infectious bursal disease virus which can circumvent vaccination with standard type I strains. J. Gen. Virol. 72:1835–1843.

13. Ismail, N. M., Y. M. Saif, W. L. Wigle, G. B. Havenstein, and C. Jackson. 1990. Infectious bursal disease virus variant from commercial leghorn pullets. Avian Dis. 34:141–145.

14. Jackwood, D. J., K. C. Cookson, S. E. Sommer-Wagner, H. Le Galludec, and J. J. de Wit. 2006. Molecular characteristics of infectious bursal disease viruses from asymptomatic broiler flocks in Europe. Avian Dis. 50:532–536.

15. Jackwood, D. J., and S. E. Sommer-Wagner. 2005. Molecular epidemiology of infectious bursal disease viruses: distribution and genetic analysis of newly emerging viruses in the United States. Avian Dis. 49:220–226.

16. Jackwood, D. H., and Y. M. Saif. 1987. Antigenic diversity of infectious bursal disease viruses. Avian Dis. 31:766–770.

17. Kaerber, G. 1931. Beitrag zur kollektiven Behandlung pharmakologischer Reihenversuche. Arch. Exp. Pathol. Pharmakol. 162:480.

18. Kunkel, T. A., J. D. Roberts, and R. A. Zakour. 1987. Rapid and efficient site-specific mutagenesis without phenotypic selection. Methods Enzymol. 154:367–382.

19. Lee, C. C., T. P. Ko, C. C. Chou, M. Yoshimura, S. R. Doong, M. Y. Wang, and A. H. Wang. 2006. Crystal structure of infectious bursal disease virus VP2 subviral particle at 2.6 Å resolution: implications in virion assembly and immunogenicity. J. Struct. Biol. 155:74–86.

20. Lim, B. L., Y. Cao, T. Yu, and C. W. Mo. 1999. Adaptation of very virulent infectious bursal disease virus to chicken embryonic fibroblasts by site-directed mutagenesis of residues 279 and 284 of viral coat protein VP2. J. Virol. 73:2854–2862.

21. Mundt, E. 1999. Tissue culture infectivity of different strains of infectious bursal disease virus is determined by distinct amino acids in VP2. J. Gen. Virol. 80:2067–2076.

22. Mundt, E., J. Beyer, and H. Müller. 1995. Identification of a novel viral protein in infectious bursal disease infected cells. J. Gen. Virol. 76:437–443.

23. Mundt, E., and H. Müller. 1995. Complete nucleotide sequences of 5'- and 3'-noncoding regions of both genome segments of different strains of infectious bursal disease virus. Virology 209:209–218.

24. Mundt, E., and V. N. Vakharia. 1996. Synthetic transcripts of double-stranded Birnavirus genome are infectious. Proc. Natl. Acad. Sci. USA 93:11131–11136.

25. Rosenberger, J. K., S. S. Cloud, J. Gelb, E. Odor, and S. E. Dohms. 1985. Sentinel Birds survey of Delmarva broiler flocks, p. 94–101. *In* Proceedings of the 20th National Meeting on Poultry Health and Condemnation. Delmarva Poultry Industry, Inc., Ocean City, MD.

26. Rosenberger, J. K., S. S. Cloud, and A. Metz. 1987. Use of infectious bursal disease virus variant vaccines in broilers and broiler breeders, p. 105–109. *In* Proceedings of the 36th Western Poultry Disease Conference. University of California, Davis, CA.

27. Saif, Y. M. 1984. Infectious bursal disease virus type, p. 105-107. *In* Proceedings of the 19th National Meeting On Poultry Health and Condemnations. Delmarva Poultry Industry, Inc., Ocean City, MD,

28. Sali, A., and T. L. Blundell. 1993. Comparative protein modeling by satisfaction of spatial restraints. J. Mol. Biol. 234:779–815.

29. Saugar, I., D. Luque, A. Ona, J. F. Rodriguez, J. L. Carrascosa, B. L. Trus, and J. R. Caston. 2005. Structural polymorphism of the major capsid protein of a double-stranded RNA virus: an amphipathic alpha helix as a molecular switch. Structure 13:1007–1017.

30. Schnitzler, D., F. Bernstein, H. Müller, and H. Becht. 1993. The genetic basis for the antigenicity of the VP2 protein of the infectious bursal disease virus. J. Gen. Virol. 74:1563–1571.

31. Schröder, A., A. A. W. M. van Loon, D. Goovaerts, and E. Mundt. 2000. Chimeras in noncoding regions between serotypes I and II of segment A of infectious bursal disease virus are viable and show pathogenic phenotype in chickens. J. Gen. Virol. 81:533–540.

32. Snyder, D. B., D. P. Lana, B. R. Cho, and W. W. Marquardt. 1988. Group and strain-specific neutralization sites of infectious bursal disease virus defined with monoclonal antibodies. Avian Dis. 32:527–534.

33. Snyder, D. B., D. P. Lana, A. P. Savage, F. S. Yancey, S. A. Mengel, and W. W. Marquart. 1988. Differentiation of infectious bursal disease viruses directly from infected tissues with neutralizing monoclonal antibodies: evidence of a major antigenic shift in recent field isolates. Avian Dis. 32:535–539.

34. Snyder, D. B., V. N. Vakharia, and P. K. Savage. 1992. Naturally occurring-neutralizing monoclonal antibody escape variants define the epidemiology of infectious bursal disease viruses in the United States. Arch. Virol. 127:89–101.

35. Spies, U., H. Müller, and H. Becht. 1989. Nucleotide sequence of infectious bursal disease virus segment A delineates two major open reading frames. Nucleic Acids Res. 17:7982.

36. Vakharia, V. N., J. He, B. Ahamed, and D. B. Snyder. 1994. Molecular basis of antigenic variation in infectious bursal disease virus. Virus Res. 31:265–272.

37. Van den Berg, T. P. 2000. Acute infectious bursal disease virus in poultry: a review. Avian Pathol. 29:175–194.

38. Van der Marel, P., D. Snyder, and D. Lütticken. 1990. Antigenic characterization of IBDV field isolates by their reactivity with a panel of monoclonal antibodies. Dtsch. Tieraerztl. Wochenschr. 97:81–83.

39. van Loon, A. A. M. W., N. de Haas, I. Zeyda, and E. Mundt. 2002. Alteration of amino acids in VP2 of very virulent infectious bursal disease virus results in tissue culture adaptation and attenuation in chickens. J. Gen. Virol. 83:121–129.